JPC – Journal of Planar Chromatography – Modern TLC (2022) 35:313–330
https://doi.org/10.1007/s00764-022-00176-2

ORIGINAL RESEARCH PAPER

Screening of orange peel waste on valuable compounds by gradient multiple development diode-array high-performance thin-layer chromatography

Bernd Spangenberg[1] · **Andrea Seigel**[1] · **Regina Brämer**[1]

Received: 2 March 2022 / Accepted: 11 May 2022 / Published online: 15 June 2022
© The Author(s) 2022

Abstract

High-performance thin-layer chromatography (HPTLC), as the modern form of TLC (thin-layer chromatography), is suitable for detecting pharmaceutically active compounds over a wide polarity range using the gradient multiple development (GMD) technique. Diode-array detection (DAD) in conjunction with HPTLC can simultaneously acquire ultraviolet−visible (UV−VIS) and fluorescence spectra directly from the plate. Visualization as a contour plot helps to identify separated zones. An orange peel extract is used as an example to show how GMD−DAD−HPTLC in seven different developments with seven different solvents can provide an overview of the entire sample. More than 50 compounds in the extract can be separated on a 6-cm HPTLC plate. Such separations take place in the biologically inert stationary phase of HPTLC, making it a suitable method for effect-directed analysis (EDA). HPTLC−EDA can even be performed with living organism, as confirmed by the use of *Aliivibrio fischeri* bacteria to detect bioluminescence as a measure of toxicity. The combining of gradient multiple development planar chromatography with diode-array detection and effect-directed analysis (GMD−DAD−HPTLC−EDA) in conjunction with specific staining methods and time-of-flight mass spectrometry (TOF−MS) will be the method of choice to find new chemical structures from plant extracts that can serve as the basic structure for new pharmaceutically active compounds.

Keywords High-performance thin-layer chromatography · Thin-layer chromatography · Orange peel extract · Gradient multiple development, GMD · Diode-array HPTLC, HPTLC−*Aliivibrio fischeri* bioassay

Abbreviations

HPTLC	High-performance thin-layer chromatography
TLC	Thin-layer chromatography
GMD	Gradient multiple development
GC	Gas chromatography
EDA	Effect-directed analysis
DAD	Diode-array detection
DART	Direct analysis in real time
TOF–MS	Time-of-flight mass spectrometry
MTBE	Methyl *tert*-butyl ether
DPPH	2,2-Diphenyl-1-picrylhydrazyl

✉ Bernd Spangenberg
Spangenberg@HS-Offenburg.de

[1] Institute of Process Engineering, Offenburg University of Applied Sciences: Hochschule Offenburg, Badstrasse 24, 77652 Offenburg, Germany

1 Introduction

Citrus is one of the most widely grown commercially crops in tropical and subtropical regions worldwide [1]. Sweet oranges (*Citrus* × *sinensis* (L.) Osbeck) are the most widely produced citrus fruits, with 70.6 million tons produced in 2012 [2]. Orange peel extract is an example of the complexity of plants containing numerous compounds. The total content of polyphenols is higher in the peel of citrus fruits, which is usually discarded, than in the peeled fruit [2]. Citrus peel is an economically valuable source of compounds because it contains significant amounts of dietary usable fibres, pectin, sugars, polyphenols such as the flavones hesperidin and naringin and polymethoxylated flavones such as sinensetin, and nobiletin, essential oils such as D-limonene, various flavonoids, carotenoids, and ascorbic acid [1, 2]. Green extraction methods [2, 3] make orange peel waste a valuable resource for sugars suitable for fermentation in bioethanol production and as a substrate for solid-state fermentation [2]. Most interesting is the extraction

of polyphenols, which can be used for the formulation of healthy products, due to their antioxidant properties [4].

For orange peel extract, a complete separation of all volatile compounds by gas chromatography (GC) [5] and all non-volatile compounds by high-performance liquid chromatography (HPLC) [6] was performed. The purpose of this work is to investigate whether such a complete analytical examination of non-volatiles can be performed by high-performance thin-layer chromatography (HPTLC). At first glance, TLC or HPTLC are not well suited to separate all non-volatile compounds in an orange peel extract, because planar chromatographic techniques show low separation numbers compared to HPLC or GC. In contrast, the advantages of TLC and HPTLC are the ease of use, parallel separations of numerous samples, simple pre- and post-chromatographic derivatization, single use of disposable plates, UV, VIS and fluorescence detection, and free choice of mobile phases. The disadvantages of TLC are mentioned in [7]. With the introduction of HPTLC in 1977 by *A. Zlatkis* and *R. E. Kaiser*, most of the problems were overcome by the use of plates with narrow particle distribution, automated sample application and the use of slit-scanners for quantification [8].

Separation of a large number of compounds using HPTLC is best performed by gradient multiple development (GMD). This is a simple gradient technique since no additional equipment is needed to perform the gradient. The same plate is developed using different solvents of increasing solvent strength. After development, the plate is dried and scanned before the next development is performed. In the past, there were only few publications dealing with GMD [9]. *Sz. Nyiredy* et al. described the separation of apolar furocoumarins in the first step, flavonoid aglycones in a second step, and flavonoid glycosides in a third step [10]. *K. Y. Lee, D. Nurok, A. Karmen* and *A. Zlatkis* used the moderately polar solvent system benzene−ethyl acetate−methanol (4:4:1, *V/V*) in a first step for the separation of lidocaine and diphenylhydantoin. In a second development with the more polar solvent system benzene−ethyl acetate−methanol−pyridine (4:2:3:3, *V/V*), the compounds procainamide, propranolol, quinidine and clozapine were separated [11]. The GMD separation of mycotoxins by *K. Y. Lee, C. F. Poole* and *A. Zlatkis* is interesting. The solvent mixture toluene−ethyl acetate−formic acid (30:6:0.5, *V/V*) was used four times for development, followed by the mixture toluene−ethyl acetate−formic acid (30:14:4.5, *V/V*). The mycotoxins sterigmatocystin zearalenone, citrinin, luteoskyrin, ochratoxin, penicillic acid, patulin, luteoskyrin, aflatoxins B1, B2, G, G2 and M2 could be separated on a single silica gel 60 plate [12].

Planar chromatography is an open technique. After separation, the plate is open to numerous staining reactions, especially effect-directed analysis (EDA), which can reveal compounds with defined bioactivity [7]. In this way, new key pharmaceutical structures can be identified. The search for compounds of pharmaceutical interest in complex extracts requires the complete separation of the constituents in conjunction with EDA. For orange peel extract, complete separation was done by using HPLC [6] and should now be performed by HPTLC to sharpen the differences and to illuminate the potential of HPTLC.

2 Experimental

2.1 Preparation of sample and standards and application on HPTLC plate

All the chemicals used were of analytical reagent grade. Sinensetin, nobiletin and tangerine were from Cayman Chemical (Ann Arbor, MI, USA). Citral was from Fluka (Buchs, Switzerland), *ß*-humulene (*ß*-caryophyllene) was from J&K Scientific (San José, CA, USA), naringenin was from MP Biomedicals (Illkirch, France), naringin and hesperetin were from Alfa Aesar (Kandel, Germany) and polyethylene glycol 600 (PEG 600) as well as formic and sulfuric acid were from Roth (Karlsruhe, Germany). Vanillin and p-coumaric acid were from Merck (Darmstadt, Germany), and ferulic acid and 2,2-diphenyl-1-picrylhydrazyl (DPPH) from Sigma-Aldrich (Steinheim, Germany). All standards had a purity of ≥ 98.0%, except for hesperetin with 95% and *ß*-caryophyllene, which is a technical product, with a purity of ≥ 90%. Methanol, ethanol, methyl *tert*-butyl ether (MTBE), toluene, and ethyl acetate were from Carl Roth (Karlsruhe, Germany), *n*-pentane, *n*-heptane, cyclohexane and sulfuric acid were from Th. Geyer (Renningen, Germany), and Al-foil silica gel 60 F_{254} plates (1.05586) and glass plates (1.15445) with a fluorescent dye, used as stationary phase (LiChrosper®), were from Merck (Darmstadt, Germany). *Aliivibrio fischeri* bacteria were purchased from Hach Lange GmbH (LCK484 LUMIS-mini), Duesseldorf, Germany. Untreated navel oranges were procured from the local market.

Standard solutions were prepared by dissolving the standards in amounts of 2 to 7 mg in 10 mL of methanol using an Orion Cahn® C-33 microbalance from Environmental Instruments (Beverly, MA, USA). An aliquot of 10.9 mg citral was dissolved in 10 mL ethyl acetate. To prepare the sample solution, the orange coloured part of the peel of a navel orange (ca. 45 g) and extracted in 45 mL of ethyl acetate for three days. (We used the peel of navel oranges because it is easy to distinguish from other oranges.) This solution was filtered and centrifuged. Due to the water in the undried orange peel, the ethyl acetate extract forms two phases. The upper phase consists of pure ethyl acetate and was used undiluted or concentrated by a factor of 5. For this purpose, an aliquot of 2.5 mL of the sample solution was evaporated to dryness with a

gentle stream of air and reconstituted with 0.5 mL of ethyl acetate.

Standard and sample solutions were spotted band-wise over 7 mm using a CAMAG Automatic TLC Sampler (ATS 4) device (Muttenz, Switzerland). Bands were spotted at a distance of 10 mm from the bottom plate edge and at a distance of 1.5 cm from the plate edges. The sample solution should be applied in amounts of 0.1 to 20 µL, because the concentrations of compounds in the sample solution vary widely.

2.2 Separation and staining

Silica gel plates (10 × 10 cm) were developed at 21 °C and 35% relative humidity in a vertical developing chamber (twin-trough glass chamber) at vapour saturation (30 min) to a distance of 60–70 mm calculated from the application. The different mixtures used as solvents were characterized as polarity ranges *A*–*G* (see Table 1). The *Vario-KS-chamber* was purchased from CAMAG and used in chamber saturation mode.

An automated "micro-droplet" spraying unit (CAMAG® Derivatizer) with unsurpassed homogeneous reagent distribution requiring low reagent consumption (2–3 mL) per plate was used for staining. The plate was sprayed with vanillin reagent (100 mg vanillin dissolved in 9.8 mL ethanol and 0.2 mL H_2SO_4) using CAMAG® Derivatizer with yellow nozzle, level 4. The plate was placed in an oven for 2 min at 100 °C. DPPH staining was performed with 2 mL of a DPPH solution (15 mg dissolved in 10 mL of methanol) using the blue nozzle, level 2.

Table 1 Separation data of the eight development steps

Polarity range	Solvent mix	Distance (mm)	Time (min)
Separation			
Focusing	Cyclohexane	10	2
A	Cyclohexane–*n*-heptane, 3:7, *V/V*	50	13
B	Cyclohexane–MBTE, 8.6:1.4, *V/V*	50	21
C	Cyclohexane–MTBE 7:3, *V/V*	60	19
D	Cyclohexane–MTBE 3:7, *V/V*	60	18
E	MBTE	60	19
F	Ethyl acetate–ethanol, 9:1, *V/V*	60	14
G	Ethyl acetate–ethanol–formic acid, 8.8:1:0.2, *V/V*	60	15

2.3 Bioautography on HPTLC plate

All the details for setting up *Aliivibrio fischeri* bacteria culture are described in [13]. The culture is ready for use after 25 to 30 h of shaking. The plate was immersed in the bacteria suspension for 6 s, and then the dipping solution was carefully wiped off with a wiper. A sensitive 16-bit CCD camera (model: Celvin® S, from biostep company, Burkhardtsdorf, Germany) was used to measure the bioluminescence within 15 min.

2.4 Mass spectrometry from plate

HPTLC zones of interest were scraped out, extracted with ethyl acetate, and then subjected to MS measurement. The DART interface from IonSense (Saugus, MA, USA) was used for HPTLC direct analysis in real-time mass spectrometry (HPTLC−DART−MS). The modified HPTLC−DART−MS system was coupled to a TOF−MS system (Jeol AccuTOFTM, Tokyo, Japan). The DART−TOF−MS operating conditions are published in [14].

2.5 Spectral measurements from plate

A TIDAS TLC S700 system from J&M (Aalen, Germany) with a reflection attachment consisting of two rows of optical fibres was used for the spectral measurements of the plate, which has a wavelength resolution of 0.8 nm and a spatial resolution on the plate of 100 µm. The measurement time for a single spectrum in the wavelength range from 190 to 1000 nm was 25 ms. For fluorescence illumination, an LED (model: LEDMOD 365.1, produced by Omicron Laserage, Rodgau, Germany) was used instead of a mercury lamp. The raw data of the measurement were evaluated using expression (1) derived from the extended *Kubelka–Munk* equation [15].

$$\mathrm{KM}(p,q) = \frac{(J_0 - J)(pJ_0 - qJ)}{JJ_0} = \frac{a}{1-a} \tag{1}$$

$$p + q = 1 \tag{2}$$

p: backscattering factor ($0 \le p \le 1$), a: absorption coefficient, J_0: reflected light intensity measured from a neat plate part, J: reflected light intensity measured from a track.

The factors p and q adapt Eq. (1) to special measurement conditions. For example, in trace analysis, not too much light is absorbed by the analyte and almost all of the illuminated light is reflected by the plate surface. This is accounted for by setting the backscattering factor p in Eq. (1) to 1, resulting in Eq. (3) [15].

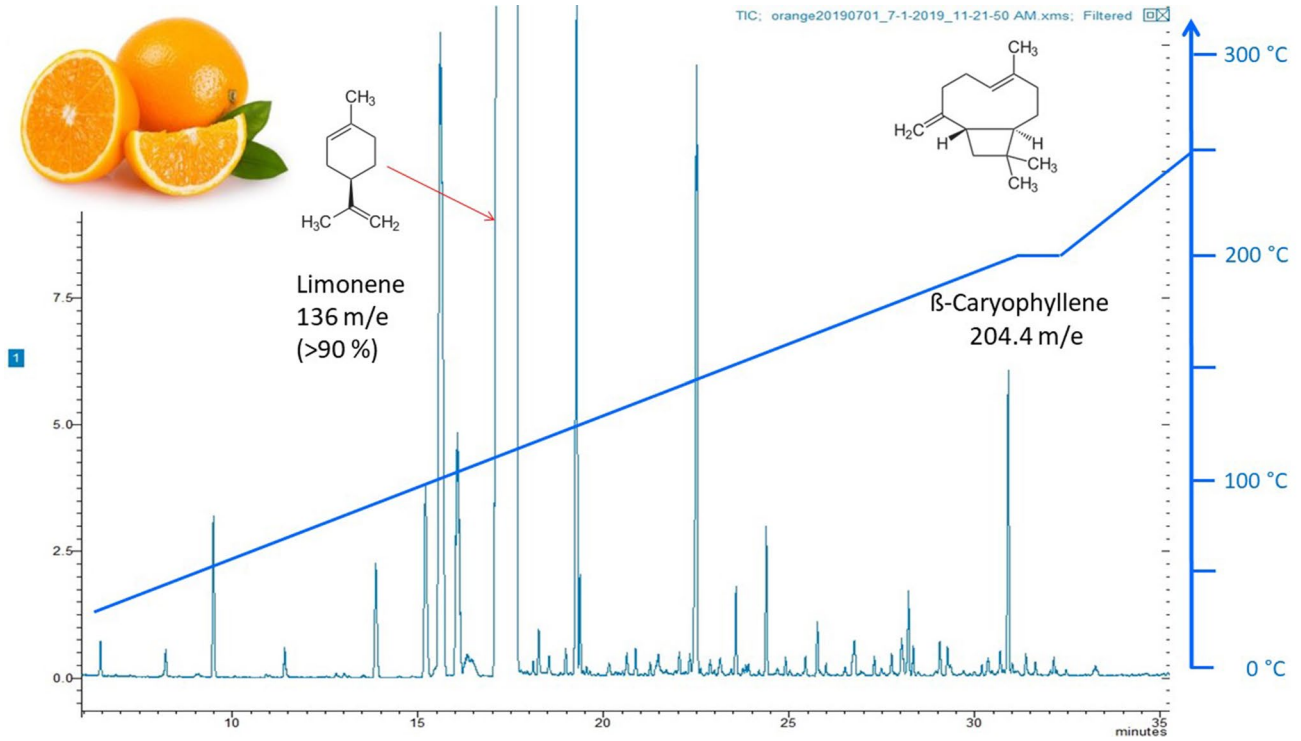

Fig. 1 Total ion GC chromatogram of an orange peel extract with overlaid temperature gradient. The major peak at 17.5 min is limonene. *ß*-Caryophyllene shows a peak at 31 min retention time

$$\mathrm{KM}(p=1)=\frac{J_0}{J}-1=\frac{a}{1-a} \tag{3}$$

In the case of fluorescence, there is no need to consider backscattering, so Eq. (1) for $p=0$ renders the desired transformation Eq. (4) [15].

$$\mathrm{KM}(p=0)=\frac{J}{J_0}-1=\frac{a}{1-a} \tag{4}$$

If the analyte is present in the stationary phase at such a high concentration that parts of the stationary phase are not illuminated by the incident light, this is corrected by a backscattering factor of $p=½$. This describes Eq. (5), which is well known as *Kubelka–Munk* equation [15].

$$\mathrm{KM}(p=1/2)=\frac{\left(J_0-J\right)^2}{2JJ_0}=\frac{a}{1-a} \tag{5}$$

2.6 Gas chromatography separation

For GC separation, the amount of 1 µL extract was separated on a 30 m column (Rxi®-5Sil MS) using a Scion SQ 436-GC–MS (Bruker, Billerica, MA, USA). The temperature gradient was 0 to 32 min 40–200 °C, 1 min at 200 °C, 33 to 40 min 200–270 °C.

3 Theory of gradient multiple development

GC measurements show that orange peel extract is a complicated mixture of many compounds [5]. This is illustrated in Fig. 1, where the amount of 1 µL orange peel extract was separated on a 30 m GC column. The chromatogram shows that the main compound in the extract is limonene (at 17.5 min separation time) with a content of more than 90%. The GC chromatogram "ends" with a strong signal at 31 min retention time, showing an *m/e* value of 204.4. This peak belongs to *ß*-caryophyllene, a natural bicyclic sesquiterpene.

The GC chromatogram in Fig. 1 shows many resolved peaks because a temperature gradient is used to vaporize the compounds over a wide temperature range from 40 to 270 °C. The compound *ß*-caryophyllene has a boiling point of 260 °C. Analysis of such high-boiling (and thus probably polar) substances by GC is limited because very high temperatures are required to move such compounds over the column. For this case, *R. E. Kaiser* recommended direct coupling of GC with TLC [16].

3.1 The solute retention factor *k*

HPTLC is an easy-to-perform separation method for the simultaneous separating of less than 10 compounds with

similar solute retention factor (k). The factor is defined as the quotient of the molar amount of substance in the stationary phase (n_s) and the mobile phase (n_m) (6) [17].

$$k = \frac{n_s}{n_m} \tag{6}$$

Any isocratic chromatographic system has its optimal resolution at $k = 2$. According to the *Martin–Synge* Eq. (7), the optimal resolution in HPTLC (for $k = 2$) is at $R_F = 1/3$ [17].

$$R_F = \frac{1}{1+k} \tag{7}$$

To achieve optimal separation of analytes, the most critical analyte pair to be separated in the system should be brought to an R_F value of 0.333, which can be easily achieved by changing the solvent composition. TLC and HPTLC can separate compounds in the R_F range of 0.1 to 0.9. According to Eq. (7), this corresponds to a k range of 9 to 0.111, which is less than two magnitudes of power. The orange peel extract contains compounds that differ in their k values by more than 10 magnitudes of power, thus cannot be separated by a single HPTLC development, *i.e.* an isocratic chromatography. For such separation problems, gradient chromatography is recommended [8–12].

In their seminal article on gradient TLC, *L. R. Snyder* and *D. L. Saunder*s point out that none of the current TLC techniques "can compete with stepwise or gradient elution from columns in terms of speed or sample resolution, when the column procedures have been fully optimized" [17]. For TLC, they do not propose a gradient technique in which compounds are compressed onto a single plate. In contrast, they propose "the separation of multicomponent samples (large range in k values) with maximum resolution (large NQ^2) is best carried out by compositing the results of several different normal TLC separations". The term NQ^2 stands for "effective plates" and describes the peak resolution capability (6) [15, 17].

$$\mathrm{NQ}^2 = \mathrm{NR}_f(1-R_f)^2 = \mathrm{NR}_f\left(1-\frac{1}{1+k}\right)^2 \tag{8}$$

The product NQ^2 is proportional to the resolution square and is called "effective plate number" [15, 17].

3.2 Focusing in HPTLC

A unique feature of multi-development in HPTLC is the mechanism of spot re-concentration [18]. After separation and drying, the current solvent front makes bottom contact with a chromatographic zone, and will bring this zone part to move first. As it passes a chromatographic zone, the solvent front narrows the zone, which is equivalent to a re-concentration. This process works against zone broadening during plate development and results in smaller and taller peaks, improving peak resolution as well as improving the limits of detection and quantification [18].

3.3 Gradient multiple development

Separation of a mixture of analytes with different k values, each of which has its optimum R_F value around 0.33, and utilization of the re-concentration mechanism is best done by GMD. For GMD, the plate is developed with different solvents of increasing solvent strength such that the least resolved analyte pair reaches a plate position of $R_F = 1/3$. After development, the plate is dried and scanned before the next development.

4 Results

4.1 Polarity range *A* (cyclohexane–*n*-heptane, 3:7, *V/V*)

The amount of 20 µL orange peel extract was focused with cyclohexane over 10 mm separation distance. After drying the plate, a separation over 50 mm was achieved in 13 min using the solvent mixture cyclohexane–*n*-heptane (3:7, *V/V*). The dry plate was scanned with the diode-array scanner in the wavelength range from 200 to 300 nm. In Fig. 2, the result is visualized under Fig. 2A. The absorption values are plotted in colour and were calculated from the measured data according to Eq. (3).

At top, the densitogram of the separation is plotted (Fig. 2B), measured at 215 nm (as an average of eleven diode signals). The UV spectrum of *ß*-caryophyllene (peak No. 1) at left (Fig. 2C) is measured in the wavelength range of 200–300 nm (spectrum averaged over nine diodes). The coloured part shows the diode-array signals of seven compounds drawn as a contour plot in the separation range from 5 to 55 mm and in the wavelength range from 200 to 300 nm. Peak 6 shows light absorption beyond 400 nm and is probably *ζ*-carotene [19]. Peak 6 was separated from the broad application zone only by the concentration step with cyclohexane.

HPTLC is a separation technique for non-volatile compounds because all volatile compounds evaporate when the sample is sprayed onto the plate. The compound *ß*-caryophyllene is the peak at 47 mm separation distance. In the system of silica gel and cyclohexane/*n*-heptane with its polar stationary and nonpolar mobile phase, *ß*-caryophyllene moves the farthest and is thus the least polar compound in the sample. When the plate is scanned several times, it can be seen that the *ß*-caryophyllene signal rapidly decreases in intensity. Therefore, it is not surprising that there are only a few articles on volatile compounds such as the liquids

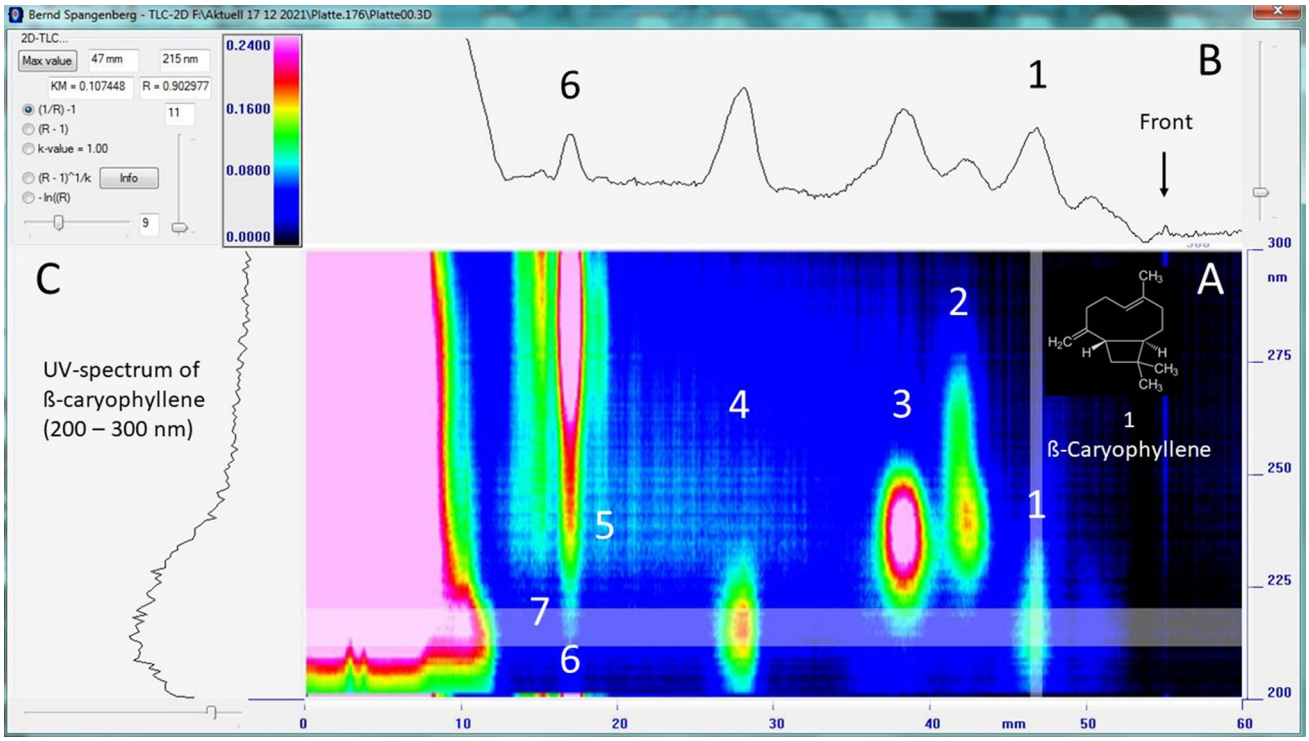

Fig. 2 HPTLC–DAD scan of an orange peel extract (**A**), separated with the solvent mixture cyclohexane–*n*-heptane (3:7, *V/V*). At top, the densitogram is plotted, measured at 215 nm (**B**). At left is plotted the UV spectrum of *ß*-caryophyllene (peak No. 1) in the range of 200–300 nm (**C**). The data were calculated according to Eq. (3)

α-humulene, *ß*-caryophyllene [20], or thujone [21] that can be separated by HPTLC. Comparing Fig. 1 with Fig. 2, one can see that HPTLC begins where GC ends.

4.2 Polarity range *B* (cyclohexane–methyl *tert*-butyl ether, 8.6:1.4, *V/V*)

The following separation with the solvent mixture cyclohexane–methyl *tert*-butyl ether (MTBE) (8.4:1.6, *V/V*) over 50 mm was achieved in 21 min without chamber saturation. An aliquot of 5 µL of the original extract was applied. The track was scanned and stained with vanillin reagent. The contour plot in the range from 200 to 400 nm is shown in Fig. 3A, above the stained track (bottom Fig. 3B). The data were calculated according to Eq. (3).

In Fig. 3, compounds 1–7 moved unresolved near the front. In the not fully resolved multi-peak (11–14), the compounds neral and geranial have been identified with neral having the lower R_F value according to [22]. Both isomers in combination are known as citral, which smells intensely of lemon. Their absorption maximum is at 250 nm, indicating a double bond in conjunction with a keto group. The compounds of peaks 9, 12 and 15 probably have a single double bond in the molecule and compounds 10 and 17 probably have two double bonds that are in conjugation. The compounds of peaks 8 and 16 show no UV absorptions. Peaks 8, 9, 12 and 16 can be stained intensely with vanillin reagent. *ß*-Caryophyllene (peak 1) and *ζ*-carotene (peak 6) can also be stained intensely, while peaks 10 and 17 show no reaction with vanillin reagent.

Figure 4 shows a separation using the same solvent system as in Fig. 3, but with 30 min chamber saturation. 10 µL of 1:5 concentrated extract was applied. In this system, the compounds of peaks 11 to 17 move to lower R_F values compared to Fig. 3, because some of the ether evaporates from the plate surface during separation. That makes it difficult to compare R_F values of different developments. The absolute values differ, but the pattern of the separated zones as well as the peak spectra is the same. This is what makes diode-array spectrometry in conjunction with a staining reaction so valuable for identifying peaks. Plate developing with or without chamber saturation is a tool that allows the R_F values to be varied within a polarity window so that selectivity can be changed.

Figure 4A shows the contour plot of a separation with the same solvent mixture as in Fig. 3, but separated without chamber saturation. The densitogram (top) was recorded at 416 nm. Below (Fig. 4B) the visible photograph of the track is shown. The peaks 8 and 9, 17–19 and 21 show intense yellow colours. The spectrum of compound 17 (Fig. 4C,

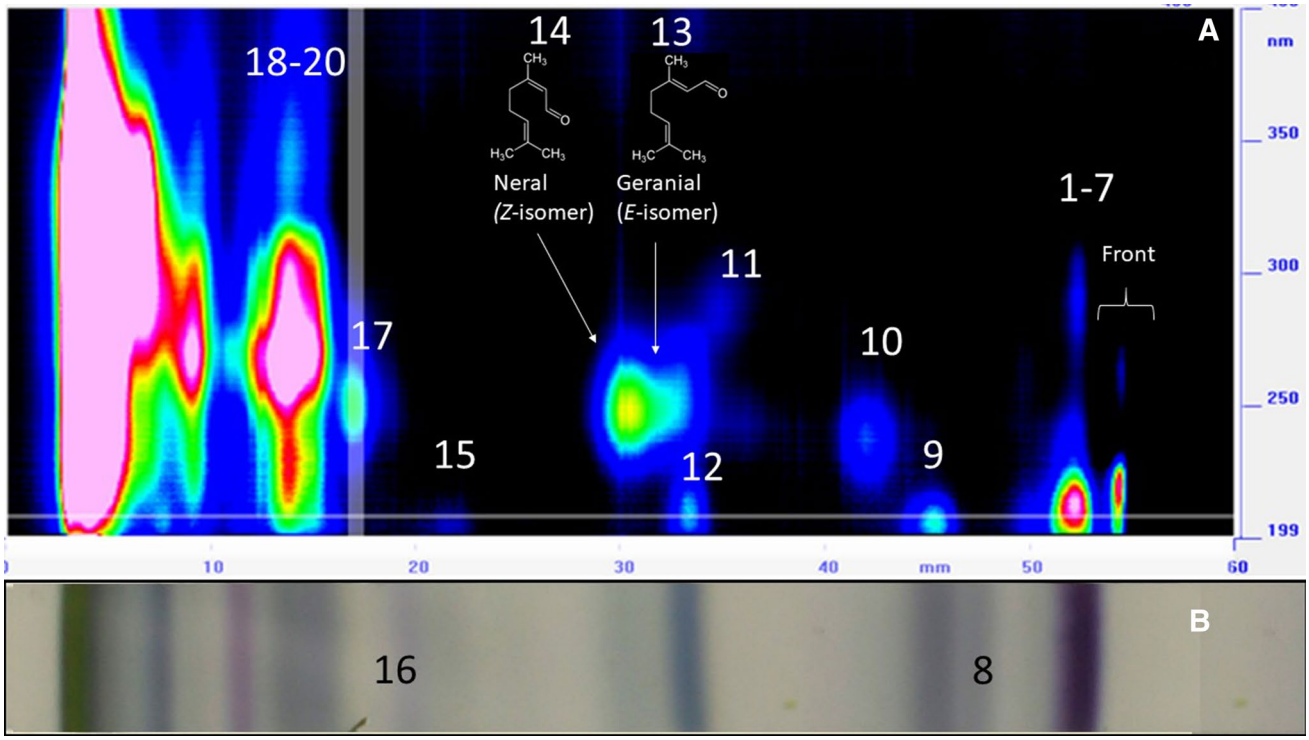

Fig. 3 Contour plot of an orange peel extract (**A**), separated with the solvent mixture cyclohexane–MTBE (8.4:1.6, *V/V*). In (**B**), the vanillin-stained track is visualized. The data were calculated according to Eq. (3)

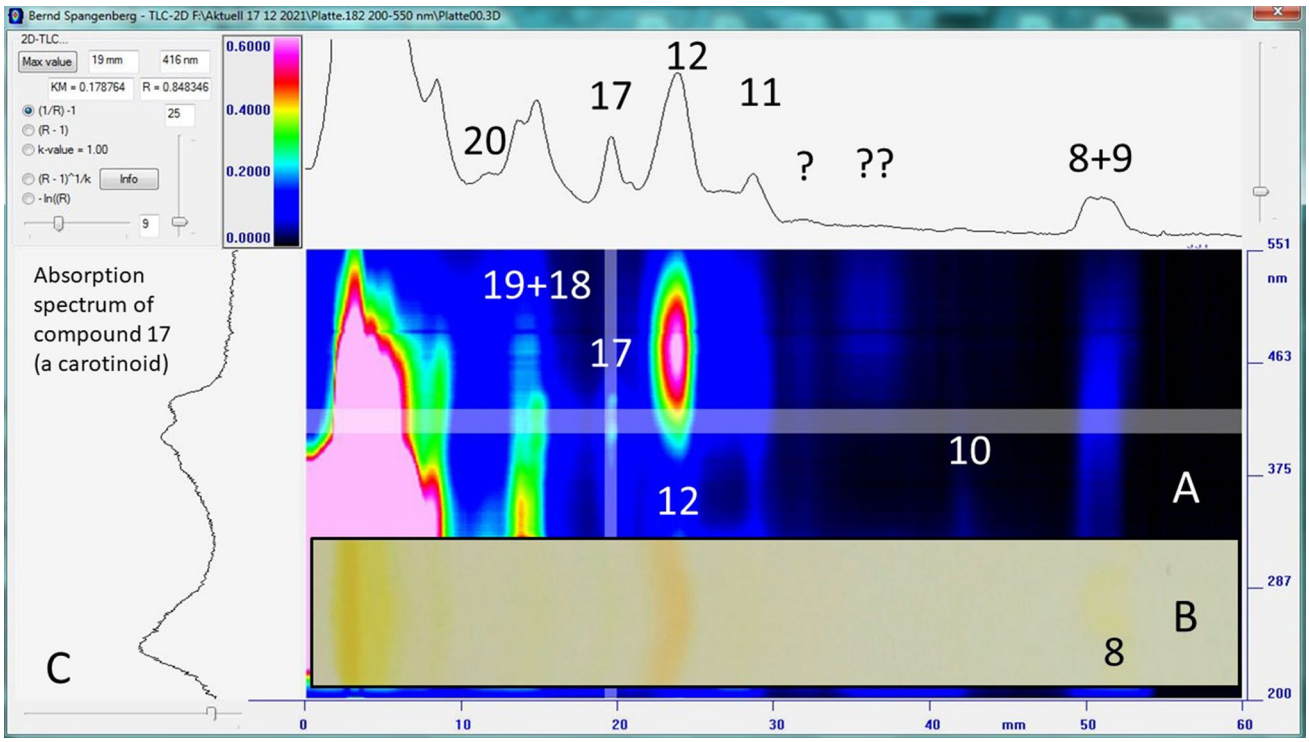

Fig. 4 **A** Contour plot with densitogram (top) recorded at 416 nm and spectrum of compound 17 (left). **B** VIS photograph of the track, separated with the solvent mixture cyclohexane–MTBE (8.4:1.6, *V/V*) without chamber saturation. **C** UV–VIS spectrum of compound 17 in the wavelength range 200–550 nm. The data were calculated according to Eq. (3)

left) shows a triplet around 400 nm typical for carotenoid [19]. Peak 12 dominates the separation with its intense orange colour. It is probably *ß*-cryptoxanthin (hydroxy-*ß*-carotene) [19]. Three other carotenoids were probably separated between peaks 10 and 11, but they do not appear in the densitogram as well as peaks 13 to 16. Additional yellow bands (probably also carotenoids) are seen near the point of application.

4.3 Polarity range *C* (cyclohexane–methyl *tert*-butyl ether, 7:3, *V/V*)

Figure 5 shows the separation over 60 mm in 19 min using the solvent mixture cyclohexane–MTBE (7:3, *V/V*). An aliquot of 5 µL of the original extract was applied on plate. Shown are the contour plot in the wavelength range from 200 to 500 nm (Fig. 5A) and the vanillin-stained track (Fig. 5B). The data were calculated according to Eq. (3).

Geranial and neral (peaks 13 and14) are well separated. Both peaks show intense signals in the contour plot, but only weakly coloured bands after staining. Between peaks 14 and 15, there appears to be an additional zone in the contour plot that has been marked "?". This signal does not show a coloured zone after staining and could not be detected in Fig. 3, probably due to its low amount. Therefore, signal was not counted as a peak.

The multiplet at 14 mm separation distance is shown in Fig. 3 (indicated as peaks 18–20), and in Fig. 5 a triplet at 30 mm separation distance is shown. This underlines that expression (8) is correct and the best resolution power is achieved at R_F values around $R_F = 1/3$. In Fig. 6, this multiplet again appears unresolved at 50 mm separation distance. Their absorptions beyond 400 nm identify the associated substances as carotenoids.

Compound 23 (in the unresolved peak 23 in Fig. 5) shows a strong red zone after vanillin staining at 20 mm separation distance. This zone can be seen in Fig. 6 at 48 mm separation distance.

4.4 Polarity range *D (cyclohexane–methyl tert-butyl ether, 3:7, V/V)*

Figure 6 shows the separation over 60 mm in 18 min using cyclohexane–MTBE (7:3, *V/V*). An aliquot of 5 µL of the original extract was applied. Shown are the contour plot in the wavelength range from 200 to 400 nm (Fig. 6A) and the vanillin-stained track (Fig. 6B).

In the contour plot in Fig. 6, the flavonoids naringenin (peak 25) and hesperetin (peak 26) can be identified. Both compounds show similar spectra with absorption maxima around 300 nm. In contrast, ferulic acid and p-coumaric acid (peaks 28 and 27) show different spectra with absorption

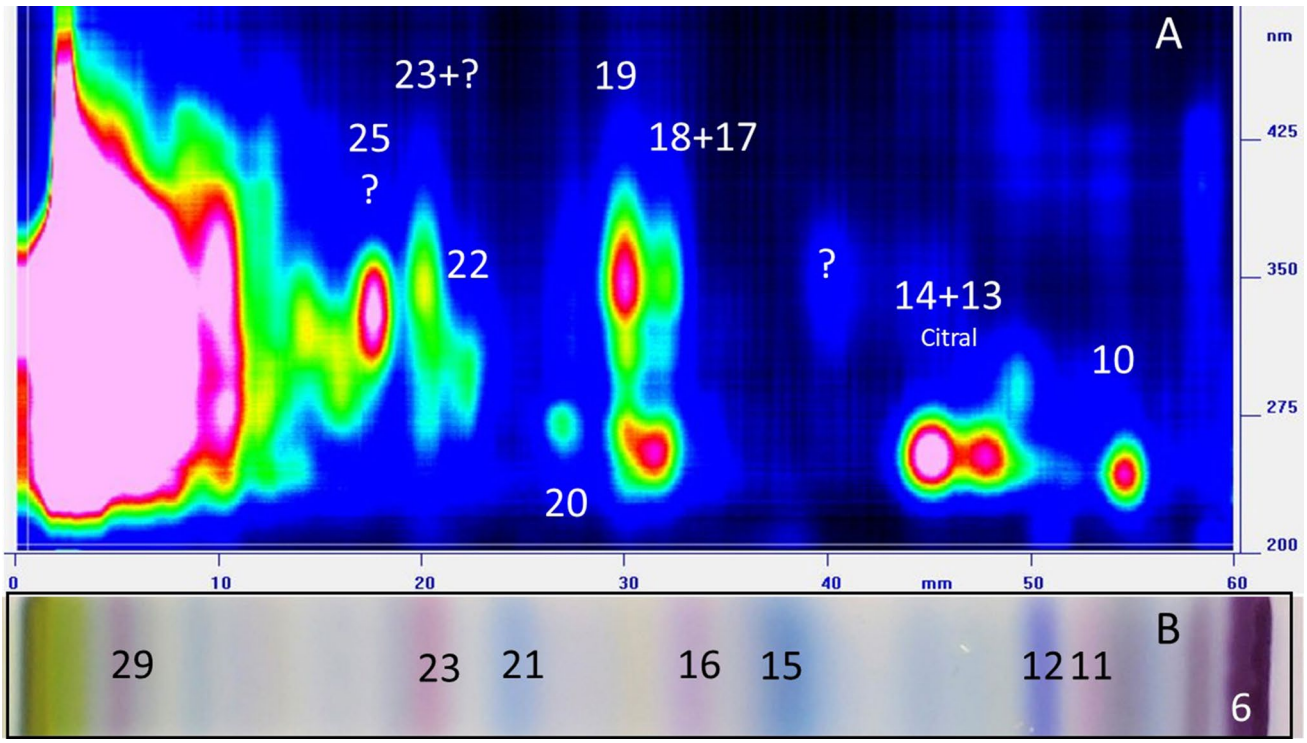

Fig. 5 Contour plot in the wavelength range from 200 to 500 nm (**A**) and vanillin-stained track (**B**) of an orange peel extract, separated with the solvent mixture cyclohexane–MTBE (7:3, *V/V*). The data were calculated according to Eq. (3)

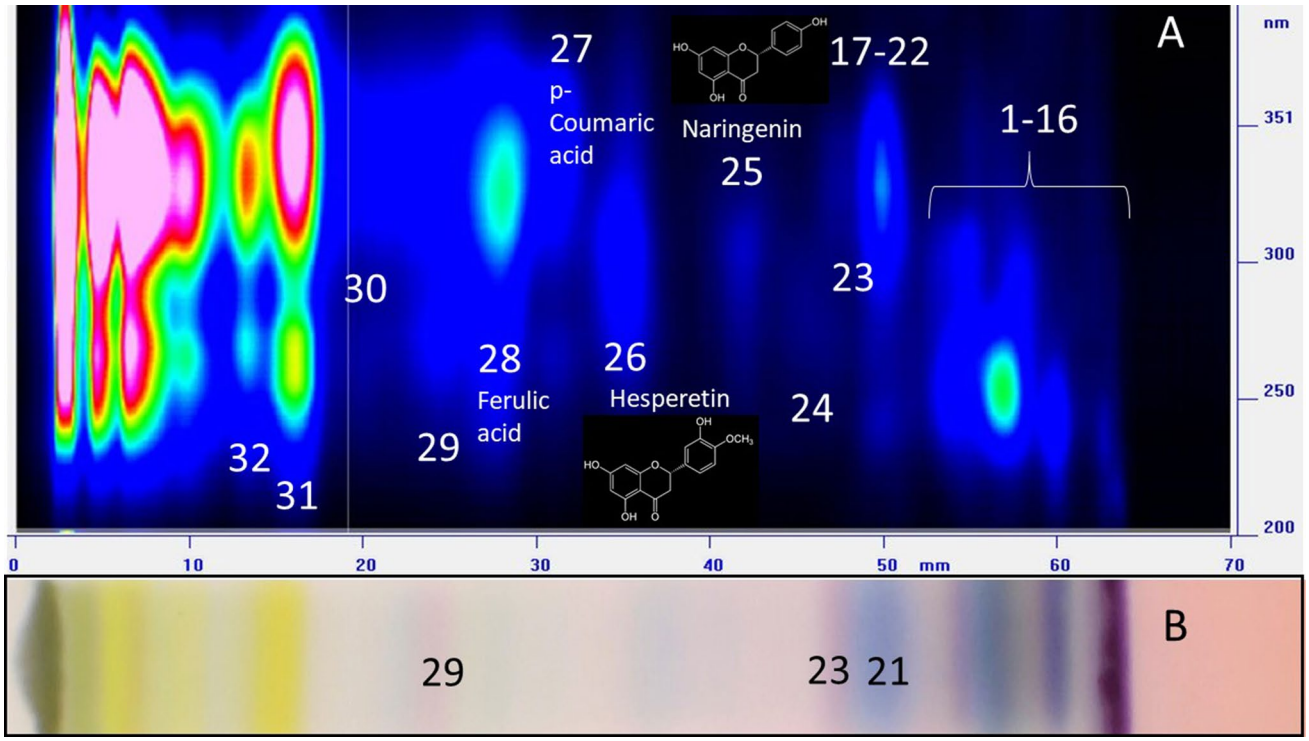

Fig. 6 Contour plot (**A**) and vanillin-stained track (**B**) of an orange peel extract separated with the solvent mixture cyclohexane–MTBE (3:7, *V/V*). The data were calculated according to Eq. (3)

maxima between 300 and 350 nm. All these compounds show only weak signals after vanillin staining. Peak 30 is the compound xanthotoxin, a coumarin derivative showing a strong fluorescence under UV 366 nm irradiation.

Below a separation distance of 20 mm, very intense signals can be seen which all have similar UV spectra and all show deep yellow-coloured zones after vanillin staining.

4.5 Polarity range *E* (methyl *tert*-butyl ether)

Figure 7 shows the separation over 60 mm in 19 min using MTBE as solvent. An aliquot of 0.5 µL of the original extract was applied. The contour plot in the range from 200 to 400 nm (Fig. 7A) is plotted below the densitogram (Fig. 7B), taken at 359 nm. The UV absorption spectrum of sinensetin (Fig. 7C) is shown on the left.

Peak 30 shows strong fluorescence and could be identified as xanthotoxin. Compared to its absorbance intensity, at least six compounds (peaks 31–36) are separated, showing much higher intensity. These group of compounds comprises by far the most abundant substances in the orange peel extract. From the mass spectra of peaks 35 and 36, it appears that these compounds are nobiletin and sinensetin, a fivefold and a sixfold methoxylated flavone, respectively. This suggests that peaks 34 and 33 are compounds 3,5,6,7,3′,4′-hexamethoxyflavone and 3',4',5,5',6,7-hexamethoxyflavone, respectively.

In orange peel juice, TLC revealed the compounds sinensetin (5,6,7,3',4'-pentamethoxyflavone), nobiletin (5,6,7,8,3',4'-hexamethoxyflavone), 3,5,6,7,8,3',4'-heptamethoxyflavone, tetra-*O*-methylscutellarein (5,6,7,4'-tetramethoxyflavone) and tangeretin (5,6,7,8,4'-pentamethoxyflavone), separated with increasing R_F values in that order [23]. In the literature, RP-HPLC separations of orange peel extracts have reported 4 to 6 compounds that have high concentrations and elute with sinensetin first [24–27]. These are the compounds sinensetin, 3',4',5,5',6,7-hexamethoxyflavone, nobiletin and tangeretin [24], sinensetin, nobiletin, tangeretin and two unidentified compounds [25], nobiletin, tangeretin, sinensetin, 5,6,7,4′-tetramethoxyflavone, 3,5,6,7,3′,4′-hexamethoxyflavone, and 3,5,6,7,8,3′,4′-heptamethoxyflavone [26], and sinensetin, nobiletin, 3,5,6,7,8,3′,4′-heptamethoxyflavone, and tangeretin [27]. In commercial orange juices, the compounds sinensetin, 3',4',5,5',6,7-hexamethoxyflavone, nobiletin, heptamethoxyflavone, tetra-O-methylscutellarein, and tangeretin were determined [28].

All this agrees well with our own result and suggests that peak 32 in Fig. 7 should be tangeretin. However, from the literature review, the question arises as to which compound is separated as peak 31. The DART–TOF–MS

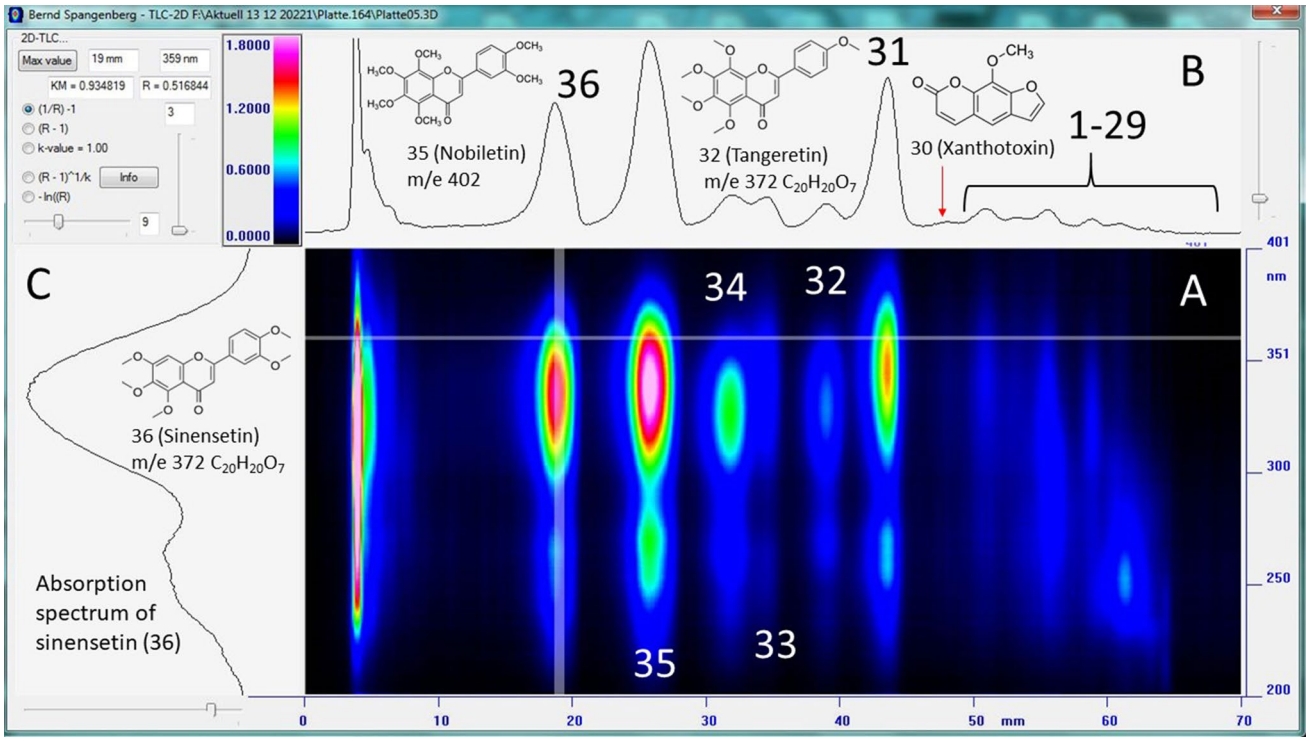

Fig. 7 Contour plot of an orange peel extract (**A**) separated with MTBE solvent. The data were analysed according to Eq. (3). At the top is plotted the densitogram (**B**), measured at 359 nm. At left is plotted the UV spectrum of sinensetin (compound No. 36) in the range from 200 to 400 nm (**C**)

spectrum (Fig. 8) of this zone shows two strong signals at 433 m/*e* and 449 m/*e*. The signal at 433 m/*e* indicates a molecule in which two C–H groups of tangeretin are replaced by two –O–CH_3 groups. This is probably the compound 3,3',4',5,6,7,8-heptamethoxyflavone. The signal at 449 m/*e* could have an additional C–OH group instead of a C–H group. The DART–TOF–MS spectrum in Fig. 8 is a clear indication that peak 31 is not pure.

It is also a strange result that the six absorption peaks in Fig. 7 show only four strong fluorescence signals, with sinensetin showing by far the most intense fluorescence. The first two fluorescence peaks correlate well with peaks 35 and 36, but the next two fluorescence signals are problematic. The third signal lies in between the R_F values of peaks 33 and 34, and the fourth fluorescence signal has its maximum at the left slope of signal 31. All this indicates that peaks 31 to 33 in Fig. 7 are not pure.

Figure 9 shows the fluorescence signals of a separation over 60 mm in 18 min using MTBE–CH_2Cl_2 (3.5:6.5, *V/V*) as solvent. Five different fluorescence signals can be seen. In Fig. 9A, the contour plot of the fluorescence signals is plotted, calculated according to Eq. (4). In Fig. 9B, the track of a tenfold higher amount obtained under UV 366 nm illumination is plotted. The densitogram is shown above, measured at 365 nm (Fig. 9C). At left, the fluorescence spectrum of sinensetin (peak No. 36) is plotted in the range from 400 to 700 nm (Fig. 9D). For illumination to generate fluorescence, a diode is used which emits light at 365 nm. The diode emits a much higher intensity of light than the detector can resolve, and thus the detector renders a saturated signal. In other words, J and J_0 have the same value. If the spectral data are evaluated according to Eq. (4), the LED signals will be rendered as zero. This can be seen in spectrum D of Fig. 9.

The fluorescence peak 34 in Fig. 9 fits well with the absorption peak of 34 in Fig. 7. The fluorescence peak 33 fits well with the absorption peak 32 in Fig. 7, and the fluorescence peak 31 fits well with the absorption peak of 31 in Fig. 7. According to the literature, tangeretin (peak 32) shows a weak yellow fluorescence [23], but this is obviously suppressed by the strong blue fluorescence of peak 33. It follows that the peak at 52 mm separation distance in Fig. 9 must contain compounds 32 and 33 and is therefore not pure. By HPTLC, we find at least six compounds with high concentration in the extract separated near sinensetin (peaks 31 to 36).

In the fluorescence contour plot of Fig. 9A, peak 31 shows a symmetrical shape and a blue fluorescence. Interestingly, a yellow fluorescent zone can be observed at higher concentrations when the plate is illuminated with UV 366 nm light. The contour plot in Fig. 9A was measured on a track where

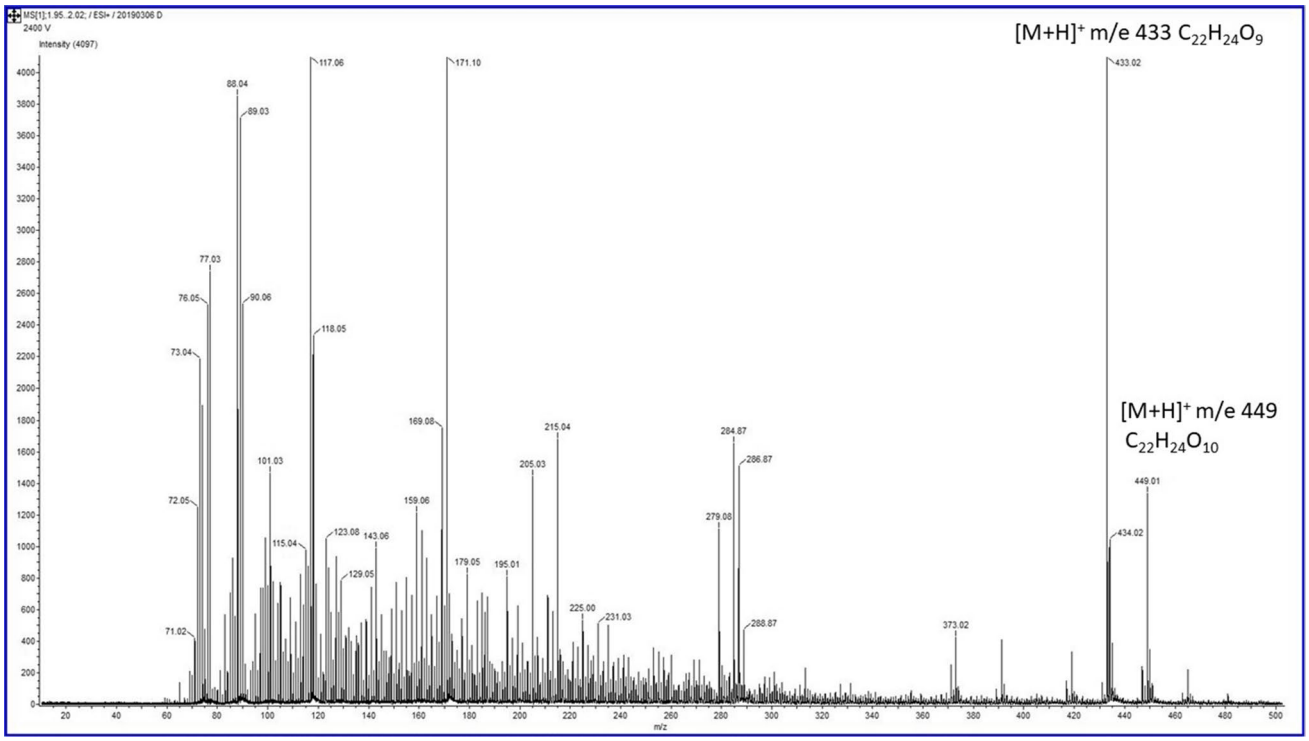

Fig. 8 DART–TOF–MS of peak 31. The signals at *m/e* 433 and 449 are interesting

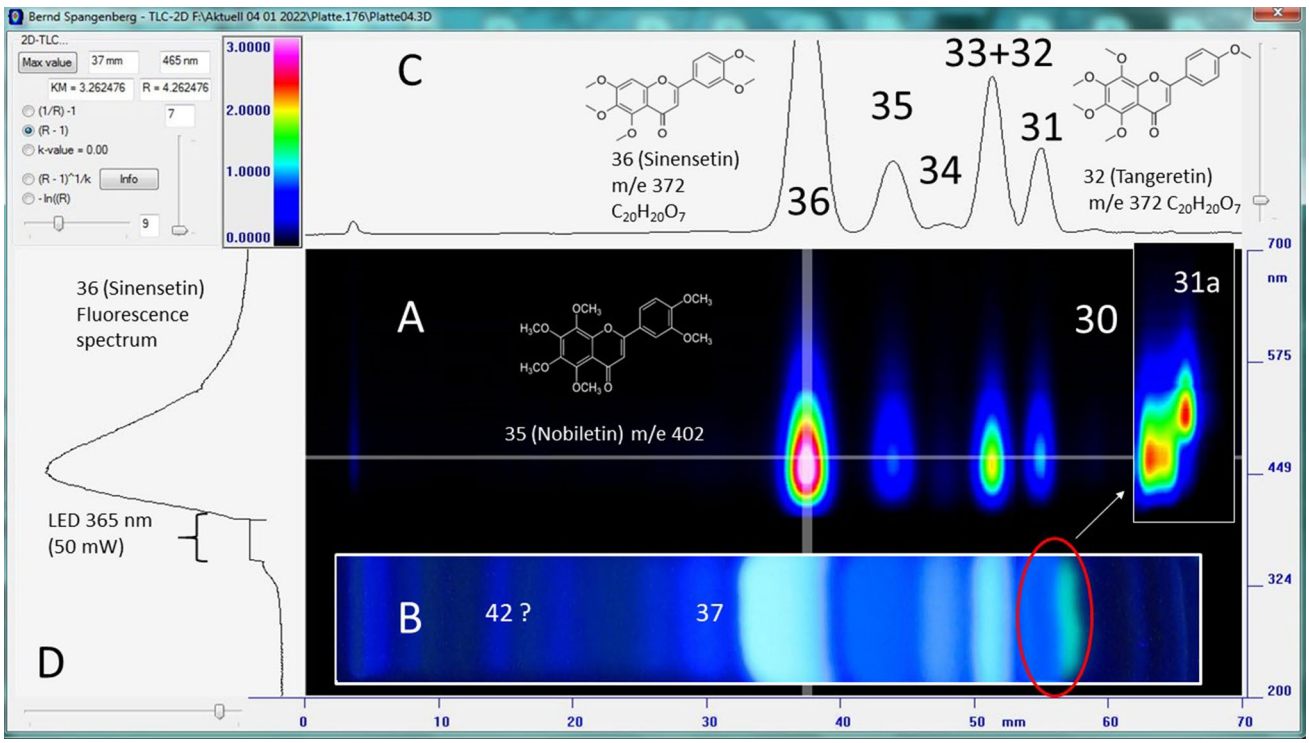

Fig. 9 Fluorescence contour plot of an orange peel extract separated with the solvent mixture MTBE–CH_2Cl_2 (3.5:6.5, *V/V*). Data were calculated according to Eq. (4). **A** Shown is the contour plot of the fluorescence signals. **B** The track of a tenfold higher sample amount, illuminated with UV 366 nm light. At the top is plotted the densitogram, measured at 365 nm (**C**). At left, the fluorescence spectrum of sinensetin (peak No. 36) is plotted in the range from 400 to 700 nm (**D**)

0.5 µL extract was separated. The track shown in Fig. 9B is a separation of 5 µL of extract. The tenfold amount of zone 31 shows a small yellow band on the right side of its blue zone that cannot be from tangeretin. The corresponding contour plot signal (31a) shows at least three peaks, with the fluorescence of the right region shifted to higher wavelengths (over 575 nm). This is a second indication that peak 31 contains different compounds.

4.6 Two-dimensional separation in the polarity range *E*

The polarity window shown in Fig. 9 (polarity range *E*) clearly contains more compounds than HPTLC can separate. In such a case, HPTLC opens the possibility to separate in a second dimension. The plate only needs to be dried and developed perpendicular to the first direction with a second solvent, which should preferably have orthogonal properties. Roughly calculated, we have separated eleven fluorescent zones in Fig. 9B. Assuming round peaks of diameter *d* and a separation number of $SN = 11$, the maximum capacity for a two-dimensional separation is 154 peaks, calculated according to Eq. (9).

$$\mathrm{SN}(2D) = \frac{4}{\pi}\mathrm{SN}^2 \tag{9}$$

Figure 10 shows a two-dimensional separation of 0.5 µL orange peel extract on a 10 × 10 cm silica gel 60 HPTLC plate. In the first direction, the plate was developed with cyclohexane–MTBE (3:7, *V/V*) over 60 mm and then with MTBE–CH_2Cl_2 (6.5:3.5, *V/V*) in 16 min. For development in the second direction over 60 mm in 13 min, the solvent mixture toluene–ethyl acetate–methanol (55:45:5, *V/V*) was used. At left and top, the standards sinensetin, nobiletin and tangeretin were separated in addition to 0.5 µL of extract each. The sinensetin standard shows three side peaks (top), nobiletin shows two side peaks (best seen at left) and the weak yellow fluorescent tangeretin shows a single contamination.

In Fig. 10, it can be seen that only spot 34 is pure, as it has no side peaks. Sinensetin (peak 36) shows two side peaks (36a and 36b), peak 33 three additional peaks (33a–c), and peak 31 shows three contaminations (31a–c). In the orange peel extract, a tangeretin (peak 32) cannot be detected under UV 366 nm because its amount is below the detection limit. Of interest is the nobiletin spot (peak 35), which appears to have only a single contaminant, detected as 35a under UV 366 illumination (Fig. 10A), but staining with vanillin (shown in Fig. 10B) reveals a second side peak (35b). In Fig. 10A, a series of fluorescent spots can be seen, starting with peak 37. In summary, there are many more methoxylated flavones present in an orange peel extract than have

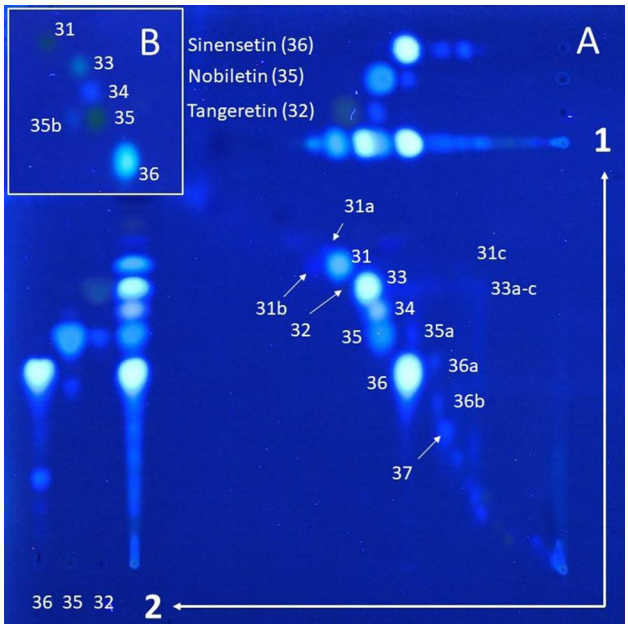

Fig. 10 **A** Fluorescence evaluation at 366 nm illumination of a two-dimensional separation. In the first direction, the plate was developed using cyclohexane–MTBE (3:7, *V/V*) and after drying was developed again with the solvent mixture MTBE–CH_2Cl_2 (3.5:6.5, *V/V*). In the second direction, the plate was developed with the solvent mixture toluene–MTBE–methanol (55:45:5, *V/V*). **B** After staining with vanillin, the plate was evaluated under UV 366 nm light

detected by HPLC and HPTLC to date. Preparative chemistry has known this for a long time [29].

4.7 Polarity range *F* (ethyl acetate–ethanol, 9:1, *V/V*)

Figure 11 shows the separation of the original orange peel extract as a fluorescence contour plot, separated over 60 mm in 14 min using ethyl acetate–ethanol (9:1, *V/V*) as solvent mixture. In Fig. 11A, the fluorescence densitogram of the separation is shown, measured at 450 nm. In Fig. 11B, the contour plot of the fluorescence signals is plotted, which was evaluated according to Eq. (4). In Fig. 11C, the unstained track is shown, illuminated with UV 366 nm light. In Fig. 11D, the track is shown after staining with vanillin reagent and measured under visible light. In Fig. 11E, the fluorescence spectrum of peak 38 is plotted, measured in the wavelength range of 400–700 nm.

In Fig. 11C, at least ten fluorescent zones can be distinguished. The two strong zones 37 and 38 are followed by two weaker zones (39 and 40), which show only two small peaks in the densitogram (Fig. 11A). Peak No. 42 is rather broad and probably consists of three unresolved peaks. In Fig. 11D, some yellow zones can be seen. These yellow zones are probably from methylated flavones. Peaks 41 and 43 will also belong to this group of compounds.

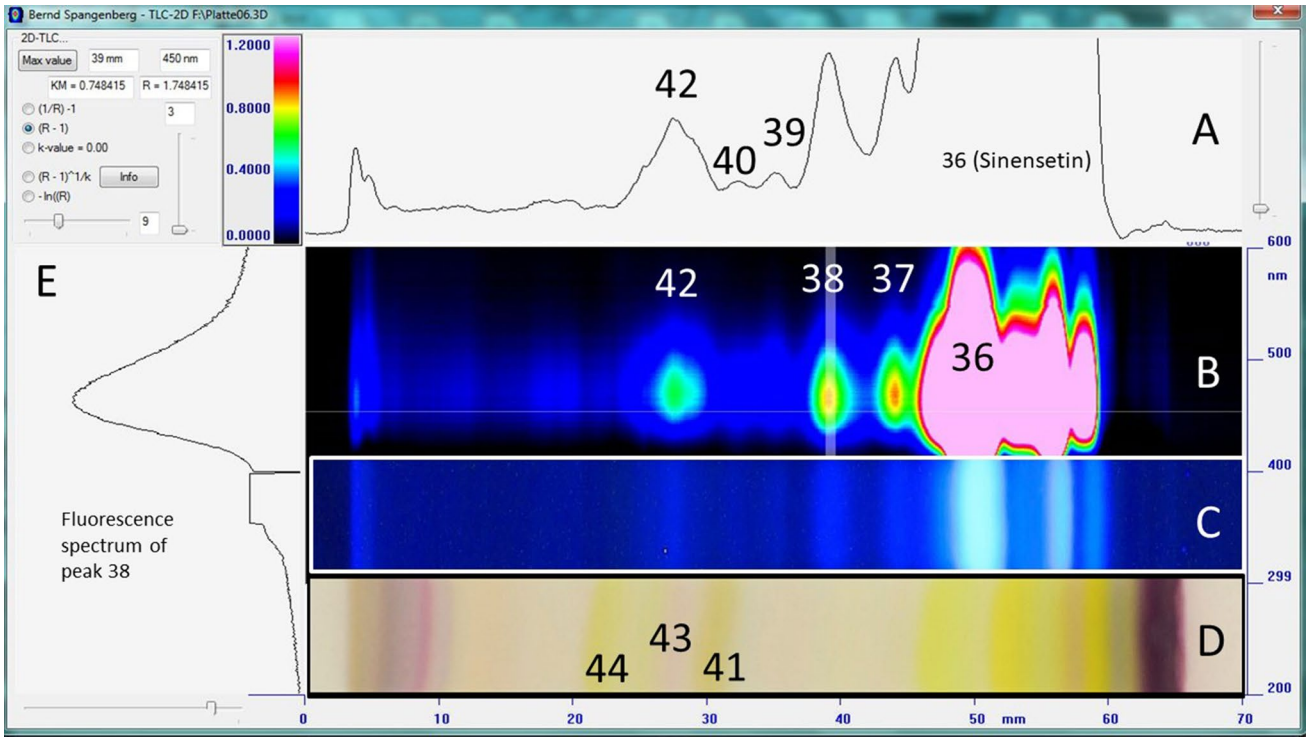

Fig. 11 Fluorescence contour plot of an orange peel extract, separated with the solvent mixture ethyl acetate–ethanol (9:1, *V/V*). Data were evaluated according to Eq. (4). **A** Shown is the fluorescence densitogram measured at 450 nm. **B** Contour plot of the fluorescence signals. **C** Track of the separation taken under UV 366 nm. **D** The track stained with vanillin reagent and measured under VIS light. E: The fluorescence spectrum of peak 38 in the wavelength range of 400–700 nm is shown at left

4.8 Polarity range *G* (ethyl acetate–ethanol–formic acid, 8.8:1:0.2, *V/V*)

Figure 12 shows the separation of 5 µL of the original orange peel extract as fluorescence contour plot over 60 mm in 15 min using the solvent mixture ethyl acetate–ethanol–formic acid (8.8:1:0.2, *V/V*). After drying, the plate was stored in NH_3 vapour for 2 min to neutralize the formic acid. The raw data were evaluated according to Eq. (5), the original *Kubelka–Munk* equation. Using this equation for spectral evaluation often results in sharper peaks [15]. In Fig. 12A, the contour plot of the absorption signals is plotted, measured in the wavelength range 200–500 nm. In Fig. 12B, the separation track of a fourfold sample amount is shown, stained with vanillin reagent. The densitogram is plotted above, measured at 343 nm (Fig. 12C), and the absorption spectrum of peak 46 is plotted on the left in the wavelength range of 200–500 nm (Fig. 12D).

In Fig. 12A, peak No. 46 dominates. In Fig. 12D, the *Kubelka–Munk* spectrum of this carotenoid is plotted in the wavelength range 200–500 nm. Only four peaks are registered between this peak and the application point (at a separation distance of 5 mm). No compound is remaining at the point of application, so the separation of polarity range *G* is the last of the GMD sequence. It is interesting to note that neither naringin nor hesperidin has been identified so far. Both compounds are flavanone glycosides with R_F values in the polarity range G of 0.27 and 0.05, respectively. Both compounds are too polar to dissolve in the upper phase of the ethyl acetate/water extract. To separate and detect all polar compounds of the aqueous phase, a second GMD sequence must be performed.

5 Discussion

5.1 Discussion on GMD separation

HPTLC provides an overview of the entire sample when a GMD separation is performed until no substance is present at the point of application. Thus, a GMD separation can cover all compounds present in the sample. From the seven GMD separations performed, it can be summarized that a peak identification can only be achieved in the R_F range of 0.15 to 0.75. This is the relevant window of separation. At smaller R_F values, the peak resolution is too low for separation, and above $R_F = 0.75$, there is a wide front range where separation is also incomplete.

Figure 13 visualizes expression (8) and shows that the best peak resolution is around $R_F = 1/3$, since the largest

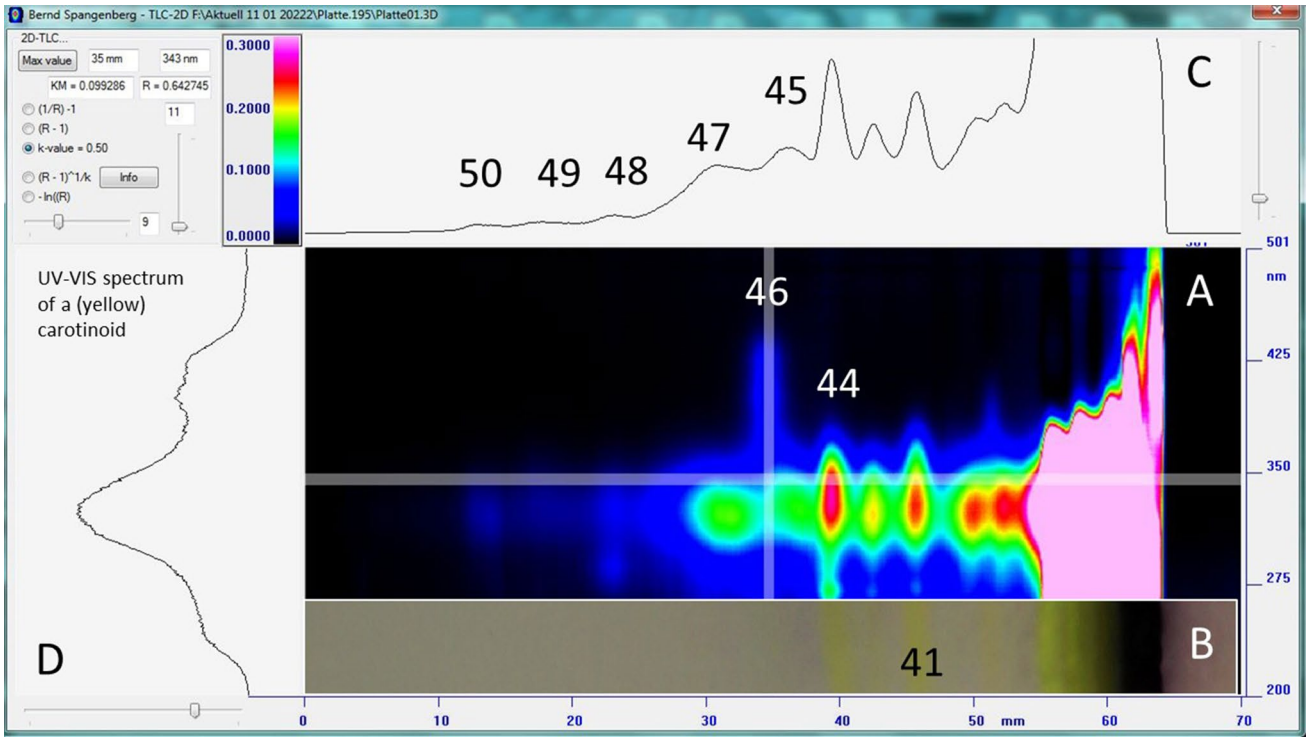

Fig. 12 *Kubelka–Munk* contour plot of an orange peel extract, separated with the solvent mixture ethyl acetate–ethanol–formic acid (8.8:1:0.2, *V/V*). The data were calculated according to Eq. (5). **A** Shown is the contour plot of the *Kubelka–Munk* signals, measured in the wavelength range 200–500 nm. **B** Separation track of a fourfold more sample amount, stained with vanillin reagent. **C** *Kubelka–Munk* densitogram measured at 343 nm. **D** The *Kubelka–Munk* spectrum of a carotenoid (peak No. 46) is plotted in the range of 200–500 nm

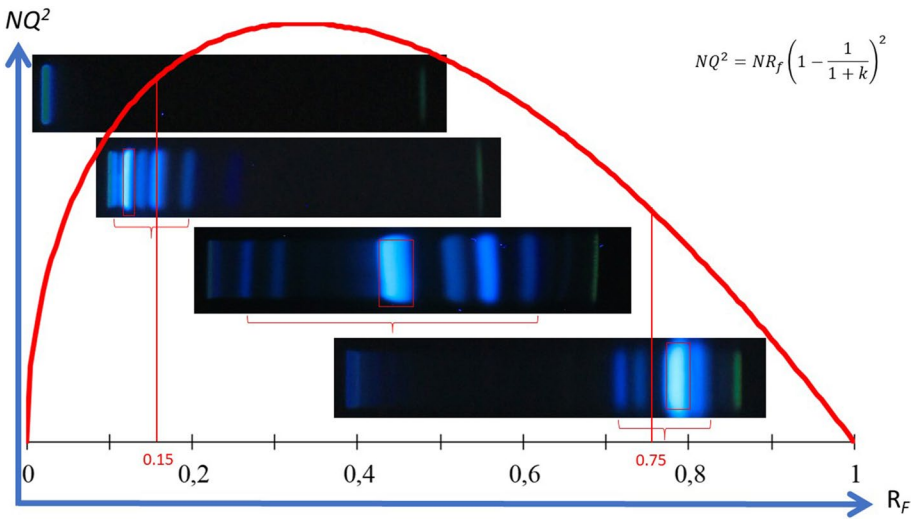

Fig. 13 Visualisation of Eq. (8) using the example of different sinensetin separations (from top to bottom the polarity ranges *A, D, E, F* are shown). The sinensetin zone is marked with a red box. The largest span of the six main blue ones is given in the R_F range from 0.15 to 0.75, so sinensetin is best separated in polarity range *E*

NQ^2 value is achieved here. The largest span of the six main blue ones is given in the R_F range from 0.15 to 0.75, GMD separation is best accomplished by selecting a new polarity window with respect to the critical peak pair to be separated next. According to expression (8), HPTLC acts like a magnifying glass through which the sample is examined. The optical magnifier shows the highest amplification around $R_F = 1/3$.

The overall analysis of a complex sample by GMD is performed by measuring overlapping polarity windows. When such polarity windows are characterized by k values rather than R_F values, Eq. (10) applies

$$k = \frac{1}{R_F} - 1 \tag{10}$$

which leads to a *k* range from 5.67 to 0.33 for the best separation. This is a log *k* range of slightly more than one order of magnitude of power. The seven polarity windows thus cover a log *k* range of more than eight orders of magnitude. Within a single polarity window, a single 6-cm HPTLC track can resolve not more than 10 to 15 peaks, whereas GMD can separate more than 50 compounds.

Running a gradient by HPLC is much more convenient than performing a GMD–HPTLC separation, but the *Vario-KS-Chamber*, introduced in 1965 by *F. Geiss*, *H. Schlitt* and *A. Klose,* facilitates the performance of GMD–HPTLC [30]. Up to six different developments on a 10 × 10 cm plate are possible, and thus six GMD tracks are available side by side on a single HPTLC plate [15, 30]. An advantage of GMD–HPTLC is that a desired polarity window can be selected directly. It is not necessary to perform a separation in uninteresting polarity ranges. For a separation in a single polarity window, a pre-separation should be performed with the solvent mixture used before the desired solvent mixture. This brings the benefit of peak focusing and results in R_F values comparable to those of a complete GMD separation.

5.2 Detection methods in GMD separations

For substance identification in HPTLC, comparing R_F values is the method of choice. With HPTLC–GMD, this is only possible within the different polarity window. More practical is the simultaneous chromatography of standards. That is maybe the reason why HPTLC–GMD is not so widely used. Diode-array HPTLC improves this situation because the absorption and fluorescence spectra of the separated zones are immediately available and can help to identify compounds and monitor how they move under different gradient conditions. Track staining in conjunction with DAD–HPTLC makes peak identification in the different polarity windows easier, because intensely stained zone can be used as a marker. In this respect, vanillin staining or staining with p-(dimethylamino)benzaldehyde was proved to be the best method.

Figure 14A shows the parallel separation of 3 µL orange peel extract, respectively, with six different solvents using the *Vario-KS-chamber.* A pre-separation was done with the solvent mixture used before developing with the desired one. As an example, track 1 (indicated as *A* + *B*) was first developed with solvent mixture *A* and, after drying, with solvent mixture *B*. To minimize peak broadening by diffusion, it is important that all developments end at the same time, so that the different development steps must be started at different times. After development, the plate was stained with DPPH to indicate substances with radical scavenger properties. Figure 14A shows the six tracks, Fig. 14B track 3 and Fig. 14C the corresponding contour plot of track 3 measured in the wavelength range 200–400 nm. The peaks 17–19 (carotenoids) and the compounds 26 (hesperetin), 28 (ferulic acid) and 32 (tangeretin) show radical scavenger properties.

5.3 EDA detection methods in GMD separations

HPTLC is the only chromatographic method where detection takes place in the stationary phase. This makes the method ideal for EDA with biological detection systems. Coupling GMD–HPTLC with biological or biochemical inhibition assays makes it possible to detect biological or toxicological active substances in situ. Enzymes or even living organism with defined bioactivity can be used for this purpose, as they remain active in the inert silica gel matrix.

Figure 15A shows the result of a single separation using the solvent mixtures *B* and *C* (Table 1), where the dried plate was dipped into a suspension of *Aliivibrio fischeri* bacteria (former called *Vibrio fischeri*). These

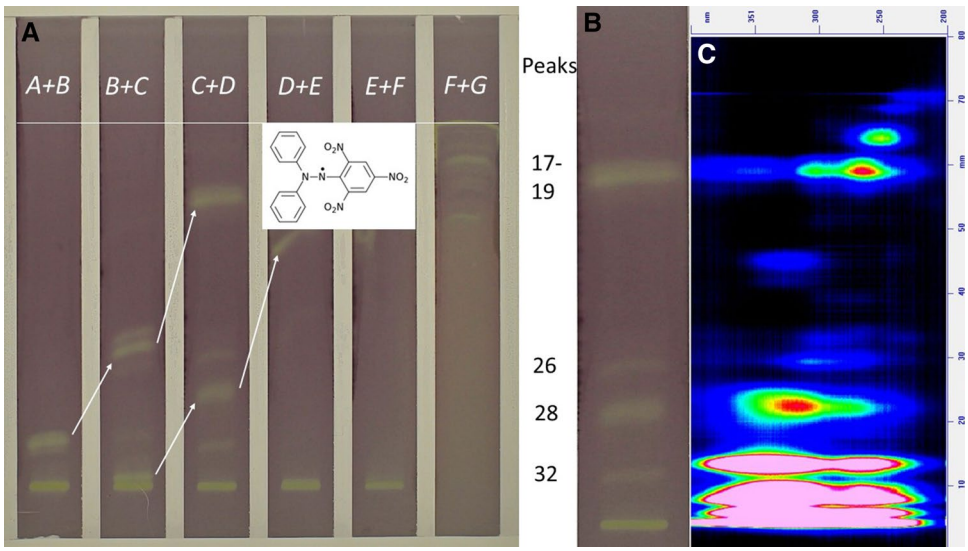

Fig. 14 **A** Parallel separation with six different solvents using the *Vario-KS-chamber* and staining with DPPH. **B** Track 3 after development with solvent mix *C* and *D* and staining with DPPH. **C** Contour plot of track 3 before staining, measured in the wavelength range 200–400 nm and evaluated according to Eq. 3

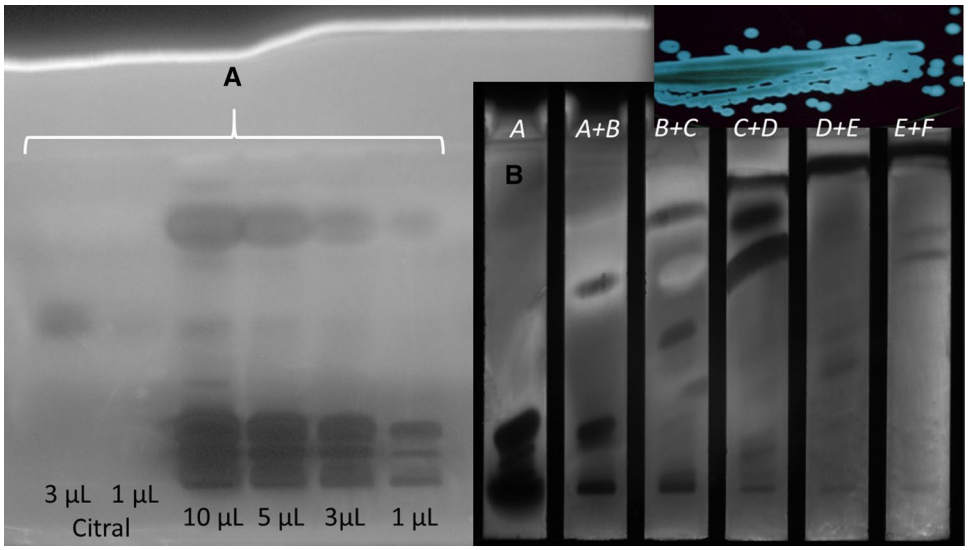

Fig. 15 **A** Separation of standard citral (3 and 1 µL), orange peel extract (10, 5, 3, 1 µL) separated with cyclohexane–MTBE (8.6:1.4, *V/V*) and immersed in *Aliivibrio fischeri* suspension. **B** Parallel separation (first track 10 µL extract, tracks 2–6 each 1 µL extract) with six different solvents using the *Vario-KS-chamber* and reaction with *Aliivibrio fischeri* suspension. The first track was developed with solvent mixture *A* only

bacteria show luminescence when active, making the plate glow in pale white light. Hazardous substances can be detected as dark zones due to the reduced or extinguished bacterial luminescence. In Fig. 15A, two tracks of a standard citral separation (3 µL and 1 µL) can be seen. The pure citral standard contains more geranial as neral. Neral seems to be more toxic to the bacteria than geranial, because here the zone is darker than that of geranial. In Fig. 15A (at right), the separation of different amounts of the orange peel extract (10, 5, 3, 1 µL) is shown. The peaks 8 and 9 (two carotenoids) show strong inhibition of *Aliivibrio fischeri,* as do the flavonoid zones near the application side.

Figure 15B shows parallel separation with six different solvents using the *Vario-KS-chamber* in conjunction with immersion in *Aliivibrio fischeri* suspension. Again, a pre-separation was performed with the solvent mixture used before developing with the desired one. The amount of 10 µL orange peel extract was applied to the first track (labelled *A*). The track was focused with cyclohexane over 20 mm separation distance. A strong bioluminescence inhibition of both carotenoids (peaks 8 and) can be seen. 1 µL of extract was applied on each of tracks 2–6. Track 3 (indicated as $B + C$) shows the separation of citral (double peak) and peaks 8 and 9 in a single band. The most intense bioluminescence suppression is seen on tracks 2 (labelled $A + B$) and 3 (labelled $B + C$) where the more apolar compound were separated. Tracks 5 and 6 show the separation of the methylated flavones. Their suppression of bioluminescence is clearly seen, but it must be considered that these compounds are present in orange peel extract in a tenfold higher concentration than citral or other apolar compound.

6 Conclusion

In 2016, it was stated [7] that "For a quantitative application in environmental EDA, TLC is less applicable due to the limited resolution, limitations in sample volumes, the qualitative nature, and the very limited selection of toxicological endpoints that may be used". To overcome these problems, *A. Zlatkis* and *R. E. Kaiser* developed HPTLC in 1977, which allows quantitative measurements and can be used for a wide range of toxicological endpoints [8]. DAD–HPTLC can simultaneously detect UV–VIS and fluorescence spectra visualized in contour plots to support the identification of separated zones. Extraction of such zones extends the analytical range and enables MS–TOF measurements.

The gradient multiple development technique, GMD–HPTLC is suitable for the determination of pharmaceutically active compounds, which was demonstrated by the example of an orange peel extract by chromatographic separation over a wide polarity range. GMD–DAD–HPTLC in seven different development steps with seven different solvents provides an overview of the entire orange peel extract. In this sample, more than 50 compounds could be separated on a 6-cm HPTC plate. HPTLC measurement takes place in the biologically inert stationary phase, making it a suitable method for EDA. GMD–HPTLC–EDA can be performed with living organism, which was confirmed by using *Aliivibrio fischeri* bacteria to detect bioluminescence as a measure of toxicity.

The combining of gradient multiple development planar chromatography with diode-array detection and effect-directed analysis (GMD−DAD−HPTLC−EDA) in

conjunction with specific staining methods and TOF−MS is the method of choice to find new chemical structures from plant extracts that can serve as the basic structure for new pharmaceutically active compounds.

Acknowledgements The authors express their appreciation to Merck Company (Darmstadt, Germany) for kind support.

Funding Open Access funding enabled and organized by Projekt DEAL.

Declaration

Conflict of interest The authors declare that they have no conflict of interest.

Open Access This article is licensed under a Creative Commons Attribution 4.0 International License, which permits use, sharing, adaptation, distribution and reproduction in any medium or format, as long as you give appropriate credit to the original author(s) and the source, provide a link to the Creative Commons licence, and indicate if changes were made. The images or other third party material in this article are included in the article's Creative Commons licence, unless indicated otherwise in a credit line to the material. If material is not included in the article's Creative Commons licence and your intended use is not permitted by statutory regulation or exceeds the permitted use, you will need to obtain permission directly from the copyright holder. To view a copy of this licence, visit http://creativecommons.org/licenses/by/4.0/.

References

1. Sharma K, Mahato N, Cho MH, Lee YR (2017) Converting citrus wastes into value-added products: economic and environmently friendly approaches. Nutrition 34:29–46. https://doi.org/10.1016/j.nut.2016.09.006
2. Putnik P, Kovačević DB, Jambrak AR, Barba FJ, Cravotto G, Binello A, Lorenzo JM, Shpigelman A (2017) Innovative "Green" and novel strategies for the extraction of bioactive added value compounds from citrus wastes—A review. Molecules 22:680. https://doi.org/10.3390/molecules22050680
3. M'hiri N, Ioannou I, Ghoul M, Boudhrioua NM (2017) Phytochemical characteristics of Citrus peel and effect of conventional and non-conventional processing on phenolic compounds: a review. Food Rev Int 33:587–619. https://doi.org/10.1080/87559129.2016.1196489
4. Fontana G (2021) The orange peel: an outstanding source of chemical resources. Citrus Res Dev Biotechnol. https://doi.org/10.5772/intechopen.96298
5. Högnadóttir Á, Rouseff RL (2003) Identification of aroma active compounds in orange essence oil using gas chromatography–olfactometry and gas chromatography–mass spectrometry. J Chromatogr A 998:201–211
6. Goulas V, Manganaris GA (2012) Exploring the phytochemical content and the antioxidant potential of *Citrus* fruits grown in Cyprus. Food Chem 131:39–47
7. Brack W, Ait-Aissa S, Burgess RM, Busch W, Creusot N, Di Paolo C, Escher BI, MarkHewitt L, Hilscherova K, Hollender J, Hollert H, Jonker W, Kool J, Lamoree M, Muschket M, Neumann S, Rostkowski P, Ruttkies C, Schollee J, Schymanski EL, Schulze T, Seiler TB, Tindall AJ, De Aragão UG, Vrana B, Krauss M (2016) Effect-directed analysis supporting monitoring of aquatic environments—An in-depth overview. Sci Total Environ 544:1073–1118
8. Zlatkis A, Kaiser RE (1977) HPTLC, high performance thin-layer chromatography. Elsevier, Amsterdam
9. Nyiredy Sz (2002) Multidimensional planar chromatography. In: Mondello L, Lewis AC, Bartle KD (eds) Multidimensional chromatography. John Wiley & Sons Ltd, Chichester, pp 171–194
10. Szabady B, Nyiredy Sz (2001) The different modes of development. In: Nyiredy Sz (ed) Planar chromatography: a retrospective view for the third millennium. Springer, Budapest, pp 88–119
11. Lee KY, Nurok D, Karmen A, Zlatkis A (1978) Simultaneous determination of antiarrhythmia drugs by high-performance thin-layer chromatography. J Chromatogr 158:403–410
12. Lee KY, Poole CF, Zlatkis A (1980) Simultaneous multi-mycotoxin determination by high-performance thin-layer chromatography. Anal Chem 52:837–842
13. Seigel A, Schröck A, Hauser R, Spangenberg B (2011) Sensitive quantification of diclofenac and ibuprofen using thin-layer chromatography coupled with a vibrio fischeri bioluminescence assay. J Liq Chromatogr Relat Technol 34:817–828
14. Peters V, Spangenberg B (2019) Equol determination in cattle manure by HPTLC-DART-TOF-MS. J Liq Chromatogr Relat Technol 42:311–316
15. Spangenberg B, Poole CF, Weins C (2010) Quantitative thin-layer chromatography. A practical survey. Springer, Berlin
16. Kaiser R (1964) Direkte und automatische Kopplung der Dünnschicht-Chromatographie an Gas-Chromatographen. Z Anal Chem 205:284–298. https://doi.org/10.1007/BF00514606
17. Snyder LR, Saunders DL (1969) Resolution in thin-layer chromatography with solvent or absorbent programming. Comparisons with column chromatography and normal thin-layer chromatography. J Chromatogr 44:1–13
18. Poole CF, Belay MT (1991) Progress in automated multiple development. J Planar Chromatogr-Mod TLC 4(3):345–359
19. Chedea VS, Kefalas P, Socaciu C (2010) Patterns of carotenoid pigments extracted from two orange peel wastes (Valencia and Navel var.). J Food Biochem 34:101–110. https://doi.org/10.1111/j.1745-4514.2009.00267.x
20. Bhramaramba A, Sidhu GS (1963) Chromatographic studies on Indian Chinnamon leaf oil. Perf Essent Oil Rec 04:732–738
21. Haznagy-Radnai E, Czigle S, Mathe I (2007) TLC and GC analysis of the essential oils of *Stachys* species. J Planar Chromatogr-Mod TLC 20(3):189–196
22. Faiyazuddin MD, Baboota S, Ali J, Ahmad S, Akhtar J (2010) Chromatographic analysis of *trans* and *cis*-Citral in lemongrass oil and in a topical phytonanocosmeceutical formulation, and validation of the method. J Planar Chromatogr-Mod TLC 23(3):233–236
23. Swift LJ (1967) TLC-spectrophotometric analysis for neutral fraction flavones in orange peel juice. J Agr Food Chem 15:99–101
24. M'Hiri N, Ioannou I, Ghoul M, Mihoubi Boudhrioua N (2015) Proximate chemical composition of orange peel and variation of phenols and antioxidant activity during convective air drying. J New Sci Agriculture and Biotechnology JS-INAT 9:881–890
25. Liu Y, Benohoud M, Hubert J, Yamdeu G, Gong YY (2021) Orfila C (2021) Green extraction of polyphenols from citrus peel by-products and their antifungal activity against *Aspergillus flavus*. Food Chem X 12(30):100144. https://doi.org/10.1016/j.fochx.2021.100144
26. Wang Z, Li S, Ferguson S, Goodnow R, Ho CT (2008) Validated reversed phase LC method for quantitative analysis of polymethoxyflavones in citrus peel extracts. J Sep Sci 31:30–37. https://doi.org/10.1002/jssc.200700331
27. Guccione C, Bergonzi MC, Piazzini V, Bilia AR (2016) A simple and rapid HPLC-PDA MS method for the profiling of citrus peels and traditional Italian liquors. Planta Med 82:1039–1045
28. Mouly PP, Gaydou EM, Arzouyan C (1999) Separation and quantitation of orange juices using liquid chromatography of polymethoxylated flavones. Analusis 27:284–288

29. Li S, Lo CY, Ho CT (2006) Hydroxylated polymethoxyflavones and methylated flavonoids in sweet orange (*Citrus sinensis*) peel. J Agric Food Chem 54:4176–4185

30. Geiss F, Schlitt H, Klose A (1965) Zur Reproduzierbarkeit in der Dünnschichtchromatographie. Z Anal Chem 213:331–346